THE JOURNAL OF PHYSICAL CHEMISTRY B

ARTICLE

pubs.acs.org/JPCB

Solubility of CO_2 in 1-Butyl-3-methyl-imidazolium-trifluoro Acetate Ionic Liquid Studied by Raman Spectroscopy and DFT Investigations

M. Isabel Cabaço,[†] M. Besnard,[‡,*] Y. Danten,[‡] and J. A. P. Coutinho[§]

[†]Centro de Física Atómica da UL, Av. Prof. Gama Pinto 2, 1694-003 Lisboa and Departamento de Física, Instituto Superior Técnico, UTL, Av. Rovisco Pais, 1049-001 Lisboa, Portugal

[‡]Institut des Sciences Moléculaires, CNRS (UMR 5255), Université Bordeaux 1, 351, Cours de la Libération, 33405 Talence Cedex, France

[§]CICECO, Departamento de Química, Universidade de Aveiro, 3810-193 Aveiro, Portugal

ABSTRACT: The polarized and depolarized Raman spectra of 1-butyl-3-methyl-imidazolium-trifluoro acetate (Bmim TFA) ionic liquid and of the dense phase obtained after introduction of supercritical carbon dioxide (313K) under pressure (from 0.1 MPa up to 9 MPa) in the ionic liquid have been recorded. The spectrum of the pure ionic liquid has been assigned by comparison with the spectra of ionic liquids sharing the same cation and using literature data concerning the vibrational modes of the TFA anion. It was found that the spectra of the ionic liquid is almost unaffected by the CO_2 dilution. The only noticeable perturbation concerns a weak enhancement of the mode assigned here to the symmetric stretch vibration of the COO group of the TFA anion. The band shape analysis of the ν_{CC} band in pure Bmim TFA shows that the carboxylate groups probe a variety of environments which are almost not affected by the dilution in carbon dioxide. The analysis of the Fermi dyad of carbon dioxide shows that this molecule is perturbed upon dilution in the ionic liquid. The spectra suggest the presence of carbon dioxide in two different environments. In the first one, carbon dioxide molecules interact with themselves, whereas in the second environment, this molecule interacts with the COO group of the TFA anion. This is supported by B3LYP-DFT calculations aimed at assessing the interaction between an ion pair dimer and a carbon dioxide molecule. It is shown that dissolved CO_2 molecules preferentially interact with the TFA anion through a weak charge transfer interaction taking place between the carbon atom of CO_2 (acting as a Lewis acid) and a oxygen atom of the COO group of TFA (as a Lewis base). The results show that Bmim TFA is able to accommodate a large amount of carbon dioxide without having its short-range local structure significantly perturbed. Most CO_2 is hosted in the voids existing among the ion pairs, while some also weakly interact with the anion. It is finally argued that the evolution of the local organization of the IL upon carbon dioxide dilution presents similarities with the microsegregation phenomena reported for IL upon increasing the alkyl chains lengths.

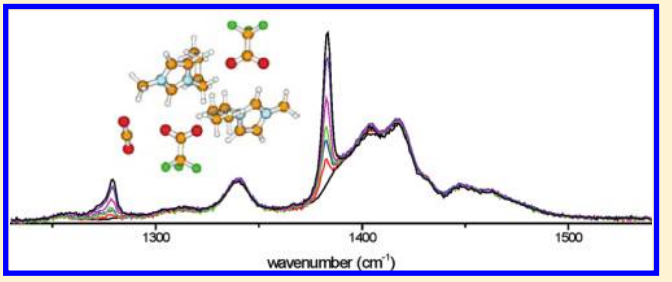

I. INTRODUCTION

Supercritical carbon dioxide is undoubtedly the widest used supercritical solvent in chemistry.[1−6] More recently, in the context of green chemistry, this fluid has attracted greater consideration by offering promising versatile attractive perspectives in the extraction processes of the products of chemical reaction performed in ionic liquids.[7−12]

Clearly, understanding interactions of carbon dioxide with organic solvents or ionic liquids is of importance in this context. For this reason, we have undertaken a series of investigations, in which we have shown that, in the dense phase of the binary mixture obtained by introducing supercritical carbon dioxide under pressure in an organic liquid solvent, the CO_2 forms transient heterodimers with the solvent molecule.[13−15] This conclusion has been reached using a combination of Raman spectroscopy and ab initio calculations allowing also to emphasize the important result that the elementary act of transient complex formation considered in the calculation matches closely the spatial and temporal spectroscopic observation conditions.

In the framework of these systematic investigations, we have recently studied the $CO_2-C_6H_6$ and $CO_2-C_6F_6$ binary mixtures.[14,15] Two motivations were at the basis of this study. The first one was connected with the field of supercritical fluid. Indeed, it has been argued that per-fluorinated fluids have a greater solvating power compared to those involving their corresponding per-hydrogenated molecule.[12,16−18] However, the molecular interpretation of this situation still has been a matter of debate as experimental or theoretical investigations in the literature bring contradictory evidence concerning the origin of the interactions at the basis of the solubility enhancement in fluorinated compounds. The second motivation of this study was the attempt to interpret the greater solubility of CO_2 in hexafluorobenzene compared to that in benzene on the ground of a complex formation. Our analysis showed that in these systems

Received: December 2, 2010
Revised: February 22, 2011
Published: March 16, 2011

transient complexes involving different charge transfer (CT) interaction are involved but that the energetic contribution in the formation of the complex, taken alone, could not explain the difference between the solubility. We showed that in fact the Gibbs energy of cavity formation represents a significant contribution to the solvation process and that the work to make a cavity capable of hosting the CO_2 molecule is greater in benzene than in hexafluorobenzene. This study has clearly pinpointed the role of energetic and entropic contribution to explain the difference of solubility of CO_2 in these hydrogenated and fluorinated solvents which can be considered as model systems.

Recently, a thermodynamical study aimed at discussing the nonideality of CO_2 solutions in ionic liquids and low volatile solvents has been published. It shows that the deviations from ideality in a broad number of systems are not related with the stability of the electron donor−acceptor (EDA) complex formed but are dominated by entropic effects.[19] Clearly, the understanding of interaction of carbon dioxide in solution is improving and consistent views are merging.

The aim of the current investigation is to study carbon dioxide diluted in an ionic liquid, namely 1-butyl-3-methylimidazolium trifluoro acetate (Bmim TFA), and to assess, at the molecular level, the nature of the interaction between carbon dioxide and the IL molecules. This system has been selected as the solubility of carbon dioxide with the pressure has been reported.[20] It is found that a large amount of supercritical carbon dioxide (313 K) can be introduced in the ionic liquid using moderate pressure as we did in our previous studies in organic solvents (see Table1). The reason for our choice is also related to the fact that the solubility of carbon dioxide in 1-butyl-3-methylimidazolium acetate (Bmim Ac) has been also reported.[20,21] However, in contrast to what it was naively expected, the solubility of CO_2 in this ionic liquid is found to be greater than that measured in the fluorinated homologue for pressures up to 4 MPa for which the CO_2 molar fraction is about 0.4. It is only at higher pressures that the solubility of carbon dioxide becomes greater in the fluorinated homologue. Clearly, we are faced with an "anomalous" type of behavior compared to that that we have investigated for benzene and its perfluorinated homologues. In this context, it is also important to emphasize that in the Bmim Ac system a peculiar behavior has been reported providing evidence of a complex formation between CO_2 and the IL with an occurring minor reversible chemical reaction of the molecules.[20,21] In contrast, neither complex formation nor chemical reaction has been reported up to now for CO_2 in Bmim TFA. The purpose of the current paper will be to investigate these questions using Raman spectroscopy and DFT modeling.

II. EXPERIMENTAL SECTION

II.1. Experimental Conditions. The Raman spectra were measured on a Jobin-Yvon HR8000 spectrometer with a Spectra Physics krypton-ion laser source operating at a wavelength of 752.5 nm with a power of 6 mW on the sample. The polarized I_{VV} and depolarized I_{HV} spectra were recorded using the backscattering geometry. Two spectral ranges, extending from 200 to 2000 cm^{-1} and 2500 to 3500 cm^{-1} in which the vibrational modes are observed, have been recorded with a resolution of 1.8 cm^{-1} using a 600 lines mm^{-1} grating. Typical spectra have been collected during 60 s and accumulated 100 times to improve the signal-to-noise ratio. In order to take accurate line positions, the spectrometer has been calibrated by recording different emission lines of a neon bulb. We have used the pressure bench and the Raman cell equipped with fused silica windows previously described[22] to work in the 0.1 to 10. MPa pressure range at T = 313 K. For the measurements in the mixtures, we initially filled the cell with the ionic liquid (Solvionic, purity greater than 98%) in order to ensure that after addition of CO_2 (Air Liquide, purity 99.995%) and pressurization the incident laser beam always impinge on the liquid phase. The mixtures were continuously stirred using a magnet activated by a rotating magnetic field. We have performed two sets of measurements. In the first one, the cell has been filled with the ionic liquid and carbon dioxide has been introduced under a pressure of 10 MPa. After an equilibration time of about 24 h, the Raman spectra have been collected. The procedure consisted of degassing the CO_2 from the cell until the selected pressure is reached and then waiting for a period of more than 2 h to allow the solution to equilibrate prior to the measurement. In the second type of experiment, we have filled the cell with the IL and introduced CO_2 under the lowest pressure to study (0.1 MPa) and allow the solution to equilibrate for more than 24 h prior to record the first spectra. Then, each stages of the measurement consisted in introducing CO_2 in the cell at increasing pressure and to allow the solution to equilibrate during more than two hours before starting the spectral acquisition. We have checked that the two procedures led, at each pressure, to reproducible results thus ensuring that the mixtures were always correctly equilibrated. The selected pressure and the corresponding molar fraction of CO_2 in the mixtures have been calculated from data reported previously[20] and are given in Table 1.

Table 1. Values of the Concentration of CO_2 in the Dense Phase of the Mixtures with Bmim TFA as a Function of the Pressure at 313 K (Interpolated from ref 20)

pressure (MPa)	CO_2 molar fraction
0.54	0.085
1.1	0.16
1.9	0.24
2.6	0.30
4.0	0.40
6.0	0.51
8.3	0.54

II.2. Experimental Results. *II.2.1. Raman Spectra of the Pure IL and Its Assignment.* The polarized I_{VV} and depolarized I_{HV} spectra of Bmim TFA neat liquid are displayed in the spectral domains mentioned above in Figure 1. To assign the vibrational modes of $Bmim^+$, we have compared the polarized spectra with those of the $Bmim^+$ BF^-_4 and $Bmim^+$ PF^-_6 ionic liquids (Figure 2) which have been studied thoroughly and for which the assignment has been reported in the literature.[23−32] A glance at this figure, in which the vibrational modes of the BF^-_4 and PF^-_6 anions have been identified and pinpointed, shows that the bands of the Bmim cation which are common to the three ionic liquids can be well identified discarding some very minor details. The values of the band center frequency extracted from this procedure agree reasonably well with the vibrational frequencies reported in the literature (Table 2). It is then a simple matter to extract the vibrational frequencies of the characteristic bands of the TFA anion which are presented in Table 2. To confirm the validity of this procedure, we have measured the Raman spectra of sodium trifluoro acetate in aqueous solution (1 mol dm^{-3}) which is presented in Figure 3 in comparison with the spectrum

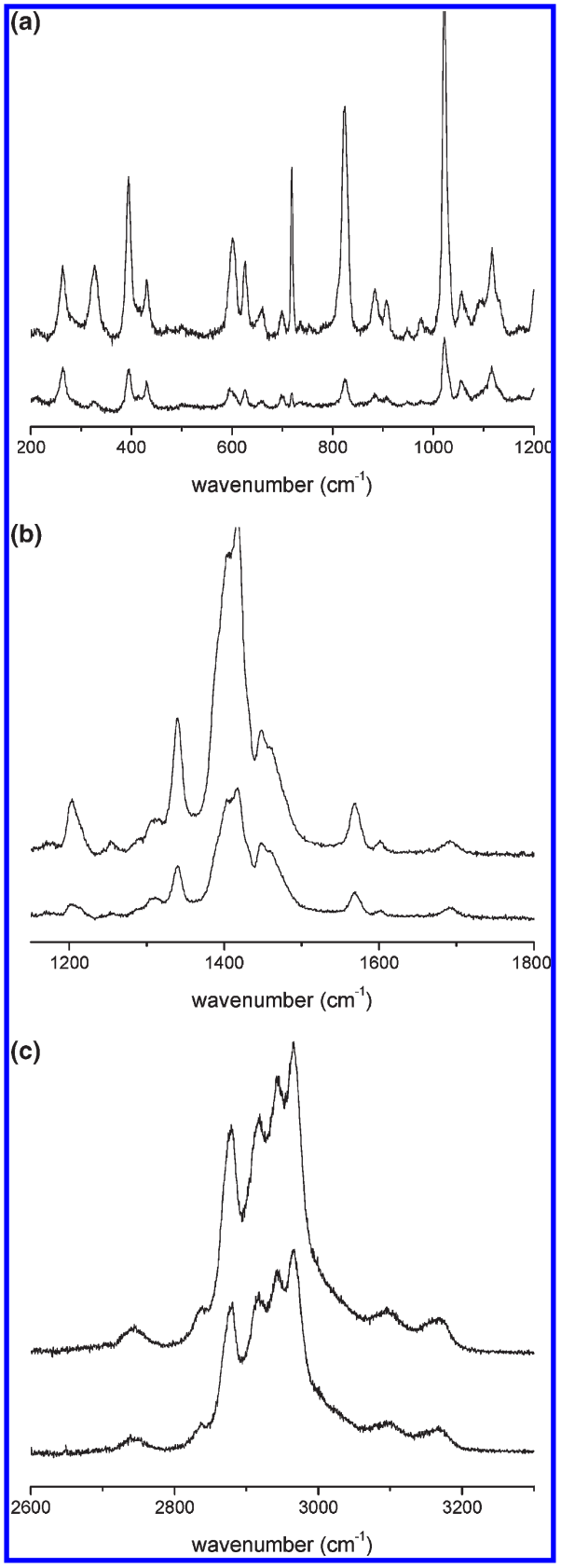

Figure 1. Polarized VV and depolarized HV Raman spectra of pure Bmim TFA. For the clarity of the representation, the spectral domain has been split into three regions.

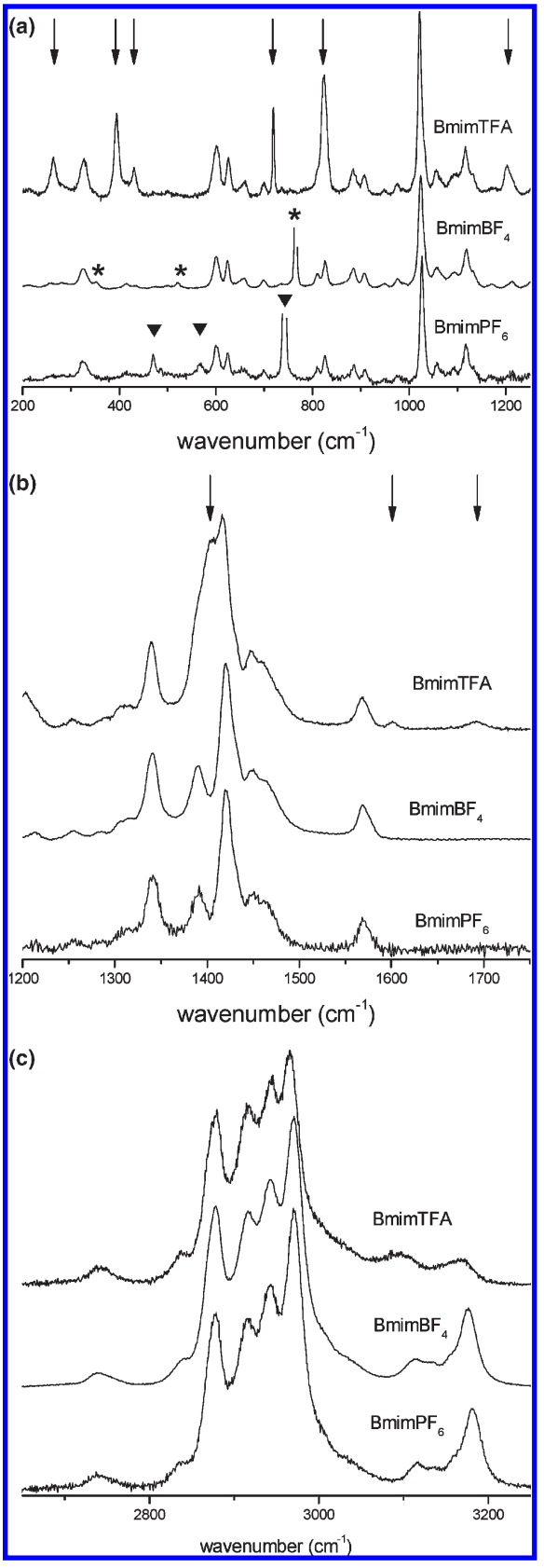

Figure 2. Comparison of the polarized Raman spectra of pure ionic liquids having the $Bmim^+$ cation in common. The bands of the anions are pinpointed for TFA^- and labeled with (★) $BF4^-$ and (▼) PF_{6^-}. For the clarity of the representation the spectral domain has been split in three regions.

dx.doi.org/10.1021/jp111453a |*J. Phys. Chem. B* 2011, 115, 3538–3550

Table 2. Tentative Assignment of the Raman Bands of the Trifluoroacetate Anion in BmimTFA and in Aqueous Solution of Sodium Trifluoroacetate (1 mol dm^{-3})[a]

TFA anion			Bmim cation	
Bmim TFA	Na TFa			
264 (D)	265 (D)	rock ⊥ CF_3		
			326 (P)	b (CH_3 (N), CH_2(N)), b CCCC
394 (D)	407 (P)	rock ⊥ CF_3		
432 (D)	435 (D)	rock ∥ CF_3		
603	599 (P)	b CF_3	601 (P)	b(ring op), ν iph (CH_2(N), CH_3 (N))
			625 (P)	b(ring op), ν iph (CH_2(N), CH_3 (N))
719 (P)	726 (P)	b OCO		
			810	ν sym (chain CC), b iph (ring (HCCH, NC(H)N op)
824 (P)	843 (P)	ν CC	825 (P)	b iph (ring HCHH, NC(H)N op), ν sym (chain CC)
			884 (P)	ν sym ($CH_2CH_2CH_3CCC$)
			908 (P)	ν sym ($CH_2CH_2CH_3CCC$)
			1020 (P)	ν (ring CN ip iph, CH_2(N), CH_2CH_3CC)
			1056 (P)	ν asym (chain CCC)
			1092 (P)	b ($(N)CH_3CH$),ν asym (ring CN)
			1117 (P)	ν sym (chain CCC)
			1132 (P)	ν (chain CC), b (butyl CH)
1203 (P)	1204 (P)	ν CF_3		
			1213 (sh)	
			1340 (P)	ν CH_3 (N), ν CH_2(N) CN, ν sym ip ring
			1389 (P)	ν CCCC
1406 (P)	1437 (P)	ν sym COO		
			1420 (P)	ν asym ip ring, ν CH_3 (N)
			1448 (P) 1462 (P)	ν sym ip ring b sym butyl HCH
			1570 (P)	ν CH_3(N), ν CH_2(N), ν asym ip ring
1602	1617[b]			
1691 (D)	1684[b]	ν asym COO		
			2741 (P)	
			2836 (P)	
			2878 (P)	ν sym CH_3HCH (terminal), ν sym CH_2C(N)HCH
			2916 (P)	ν asym butyl HCH
			2942 (P)	ν sym CH_3(N) HCH
			2965 (P) [c]	ν asym propyl HCH
			3097 (P) [d]	ν asym CH_3(N)HCH, ν ring NC(H)N CH [f]
			~3165 (P) [e]	ν sym ring HCCH, ν NC(H)N CH [f]

[a] The assignment of bands of the cation taken from literature is also reported.[23−32] P-polarised and D-depolarised profiles; rock ⊥ and rock ∥, rocking perpendicular and parallel to the CCOO plane; b, bending; ν stretching; sym and asym, symmetric and asymmetric vibrations, respectively; ip and op, in-plane and out-of-plane; iph and oph, in-phase and out-of-phase vibrations, respectively. [b] Bands contributing to the broad feature observed in the domain of the water bending. [c] ~2970 cm^{-1} for $Bmim^+$ PF_6^- and $Bmim^+$ BF_4^-. [d] ~3120 cm^{-1} for $Bmim^+$ PF_6^- and $Bmim^+$ BF_4^-. [e] ~3175 cm^{-1} for $Bmim^+$ PF_6^- and $Bmim^+$ BF_4^-. [f] This assignment is commonly accepted, however it has been revisited recently and a new kind of assignment has been proposed: [e] is assigned to the ν iph $C_{(4,5)}$ H, ν $C_{(2)}$H and ν oph $C_{(4,5)}$ H modes and [d] is assigned to overtones and combination of the ring modes in Fermi resonance.[30−32]

of Bmim TFA. It is readily apparent that the bands pinpointed to the TFA anion in Figure 2a,b are indeed observed in the spectrum of the aqueous solution. However, we note that there is a perturbation of the bands position of the anion on going from the solution to the ionic liquids. This could be anticipated as being due to the existence of a different counterion. We notice that the frequencies of the bands of the anion observed in the aqueous solution are in good agreement with the spectrum reported in the literature under similar conditions[31] (Table 2). We have then proceeded to the assignment of the bands of the anion in the IL using existing literature reported for the Raman spectra of sodium trifluoro acetate dissociated in aqueous solution[33,34] and in solid phase[35−37](Table 2).

Because the stretching vibrations of the carboxylate group play a relevant role in this study (see next section) we have performed further measurements using absorption infrared (IR) spectroscopy in this particular domain to remove any doubt on their assignments. The comparison with infrared spectra shows that bands assigned to the symmetric and asymmetric COO^- modes are clearly observed (Figure 4). The asymmetric mode which has a strong IR activity is immediately identified at 1688 cm^{-1} whereas the symmetric mode, less active, gives rise to the band

dx.doi.org/10.1021/jp111453a |J. Phys. Chem. B 2011, 115, 3538–3550

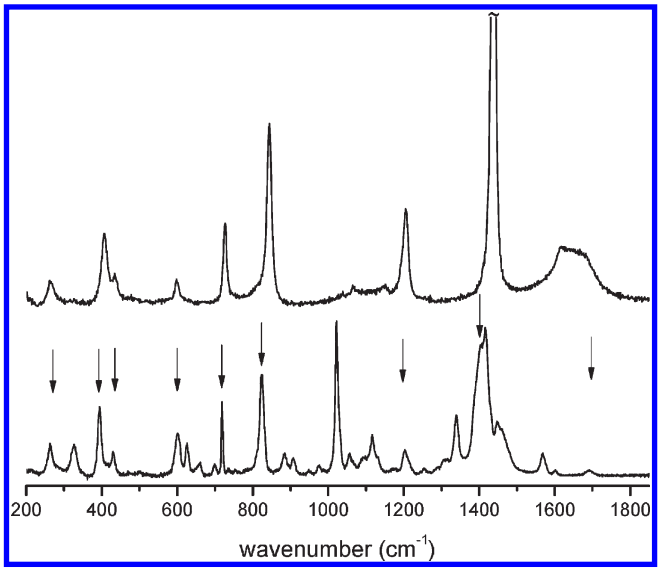

Figure 3. Comparison of the polarized Raman spectra of Bmim TFA and sodium trifluoroacetate aqueous solution (1 mol dm^{-3}).

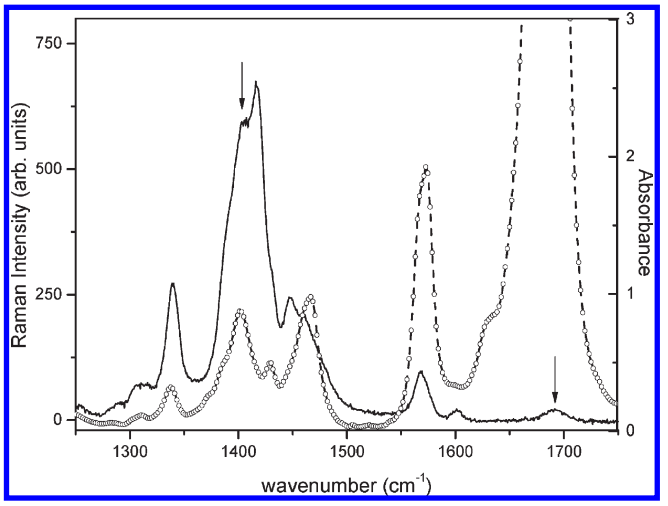

Figure 4. Comparison of the Raman (solid line) and infrared (●) spectra of Bmim TFA in the region of the carboxylate stretching vibrations.

detected at 1406 cm^{-1}. The comparison with Raman illustrates nicely the complementarity of the two techniques. Indeed, in this spectroscopy, the symmetric mode appears more intense than the asymmetric one and it is noticeable that both modes are detected at the same frequency as the IR ones.

II.2.2. Spectra of the Mixture CO_2 in Bmim TFA. The spectra of pure Bmim TFA and Bmim TFA submitted to the greatest pressure of carbon dioxide (8.3 MPa) are displayed in Figure 5. It is readily apparent that, within experimental uncertainties, the spectra of the ionic liquid is extremely weakly affected by the dilution on going from the pure IL to a binary mixture in which the molar fraction of CO_2 is about 0.54. The weakness of this effect is clearly seen on the spectra resulting from their subtraction (bottom of Figure 5).The only noticeable feature on the spectra of the ionic liquid (Figure 5) corresponds to a weak enhancement of the band situated at 1406 cm^{-1}, assigned to the symmetric stretching of the COO mode of the trifluoro acetate anion (Figure 2b and Table 2). The

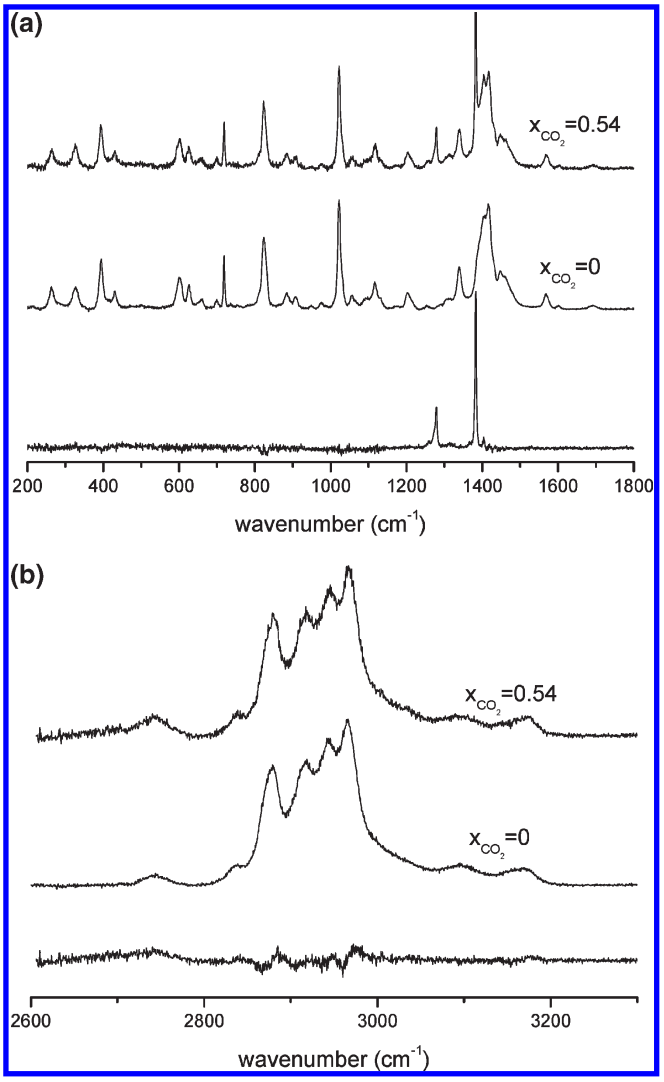

Figure 5. Comparison of the polarized Raman spectrum of pure Bmim TFA with the spectra of its binary mixture with carbon dioxide at the highest molar fraction studied (x_{CO_2} = 0.54). The difference between these spectra is reported beneath. For the clarity of the representation the spectral domain has been split in two regions.

new features clearly observed concern the two peaks centered at about 1278 and 1382 cm^{-1} having their intensity increasing with the CO_2 concentration (Figure 5a) and which can be therefore assigned to the ν_1-$2\nu_2$ Fermi doublet of carbon dioxide.[13−15] The evolution of the spectra with the CO_2 concentration restricted to this relevant spectral domain is presented in Figure 6 which shows the continuous enhancement of the dyad peaks as well as that of the band associated with the symmetric stretching mode of the COO group. We have compared these spectra with that of pure CO_2 at a density close to that of the more concentrated mixture in carbon dioxide (x_{CO_2} = 0.54). In the absence of measurements of the density of this mixture, we have crudely estimated its value at 850 kg m^{-3} under the assumption of an ideal mixture (hypothesis rather justified at posteriori, vide infra). Therefore, the spectra of CO_2 in the mixture have been compared with the spectrum of pure CO_2 measured at 22 MPa and 313K for which the density is ρ = 857.2 kg m^{-3}.[38] Figure 6 clearly shows the sizable difference (shift and broadening) experienced by the Fermi doublet of carbon dioxide on going from the pure state to the mixture. Finally, we note that in the spectral

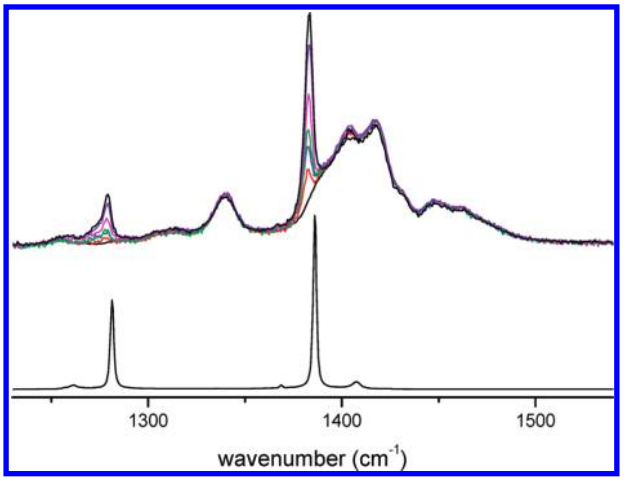

Figure 6. Evolution of the polarized Raman spectra of the Bmim TFA mixtures with increasing concentration of carbon dioxide (molar fraction of CO_2: 0, 0.16, 0.24, 0.30, 0.40, 0.51, 0.54, from bottom to top) in upper part of the figure. The polarized spectrum of pure CO_2 (22 MPa, ρ = 857.2 kg m^{-3}) is displayed for comparison in the lower part of the figure.

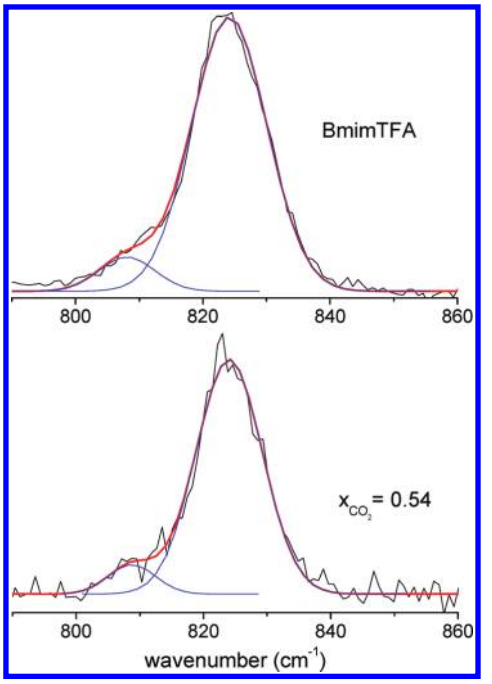

Figure 7. Isotropic Raman spectra of the ν_{CC} band in pure Bmim TFA and in the more diluted solution (x_{CO_2} = 0.54) fitted by a single Gaussian profile. The lower frequency profile describes a Bmim band centered at about 809 cm^{-1} (see Table 2).

domain, ca. 650 cm^{-1}, the presence of rather strong bands of the IL hamper the detection of any very faint feature which might be assigned to the signature of the perturbed bending mode of CO_2 (Figure 5a).[13−15]

II.3. Discussion of the Experimental Results. These experimental results show that although the IL is able to host a fairly large amount of carbon dioxide its presence induces few perturbations on its spectrum. We have thus studied the spectra of carbon dioxide in the solution to obtain further clues about the interaction between the IL and its guest CO_2 molecule. This viewpoint is particularly highlighted from a study of the ν_{CC} vibration of the anion which gives rise to an intense polarized band situated at about 824 cm^{-1}. This band has been extensively studied by Raman spectroscopy for acetate salts in aqueous solutions.[39−42] It has been shown that the ν_{CC} mode is a particularly good probe of the complexation of the carboxylate group, with sometimes more sensitiveness than the vibrations of the COO group itself. As a matter of fact, the contributions of "free", mono and bicomplexed forms of acetate ions in solution have been put in evidence from the band-shape analysis associated with this mode. In pure Bmim TFA, we found that the isotropic Raman profile I_{iso} of the ν_{CC} band ($I_{iso} = I_{VV} - {}^4/_3 I_{HV}$) could be nicely fitted using a single Gaussian profile (Figure 7). It is noteworthy that adjustments performed using Lorentzien profiles are only able to reproduce the experimental band-shape if a large number of components are considered (at least four) but still with a poorer quality than the fit obtained with a single Gaussian profile. Upon dilution of the ionic liquid with CO_2 neither the band-shape nor the band center of the experimental profiles were found to vary. This is clearly seen in Figure 7 where we have compared the experimental profile measured at the highest dilution investigated with that of the pure IL. We may therefore conclude that the ν_{CC} band-shape, as observed in the pure IL, is only very little affected by the dilution effect as testified by the fact that the value of the band center position and width of the single Gaussian profile remain almost the same.

The previous results suggest that in the neat ionic liquid, the carboxylate group of the anion interacting with the Bmim cation cannot be considered, on the Raman time scale of observation, as forming well-defined specific isolated entities (i.e., monodentate or bidendate complexes) as existing in aqueous acetate solutions. Indeed, in the latter systems, the Raman profile associated with the ν_{CC} vibration is found either to show a partially resolved structure due the presence of the different "complexes" or a band-shape in which several components associated with these species can be disentangled by a proper band-shape analysis. In contrast, in the pure IL, the observed Gaussian isotropic profile is interpreted as resulting from an inhomogeneous distribution of vibrational frequencies of the ν_{CC} mode which is sensitive to the variety of possible environments probed by the carboxylate group. Moreover, this inhomogeneous distribution suggests that the interactions between the carboxylate groups of the different anions with the Bmim cations are not drastically different one to each others.

Upon dilution with carbon dioxide, this conclusion remains still valid as seen from the fact that the band-shape of the ν_{CC} mode does not change. Hence, we are led to conclude that even if the structural organization of the IL is undoubtedly disrupted by the introduction of carbon dioxide in the IL, in particular at highest dilution, the variation of concentration is not reflected in the ν_{CC} band-shape. The significance of this result can be appreciated by reminding that the local structural organization of the IL is based minimally upon ion pair dimers.[43,44] Isolating these entities in shells of carbon dioxide does not drastically modify the interaction between the carboxylate of the anion with the Bmim cation even if weak perturbations of the COO group could be nevertheless put in evidence upon dilution. It should be stressed that the picture coming out from these results is consistent with two major outcomes on IL. The first one is based upon the fact that the "basic structural unit" of neat IL involves at least ion pair dimers as it has been previously reported.[43−49] The second one is based upon an analogy with the segregation phenomenon reported in MD

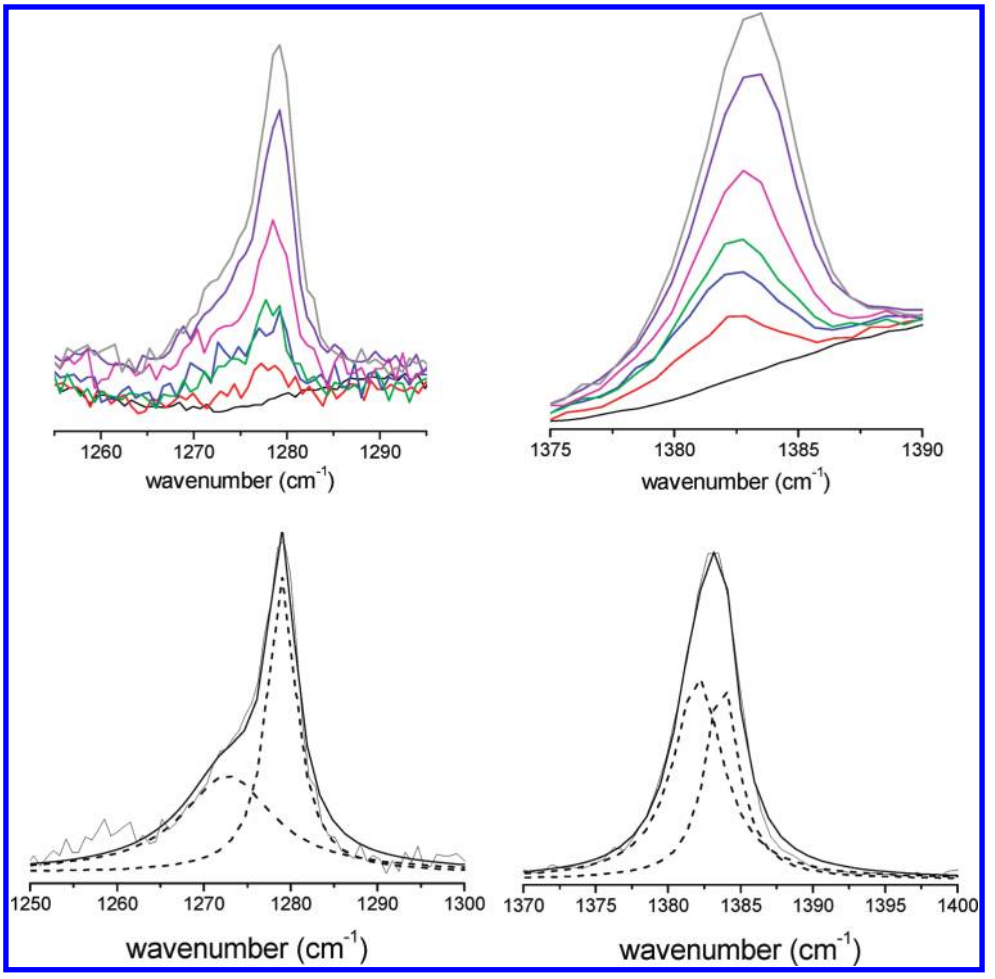

Figure 8. Top: Raman spectra of the Fermi dyad of carbon dioxide diluted in Bmim TFA at increasing molar fraction of CO_2 (bottom to top: 0, 0.16, 0.24, 0.30, 0.40, and 0.51). Bottom: Analysis of the band-shape of the dyad. Two Lorentzian profiles (dash lines) are fitted on each peak of the doublet (x_{CO_2} = 0.54).

studies of IL. It was shown that upon increasing the length of the alkyl chain, non polar domain become larger and more connected causing swelling of the ionic network.[50] Here the role of the increasing alkyl chain is played by the increasing concentration of carbon dioxide. In the Bmim TFA−CO_2 system, the CO_2 molecules are mostly encountered aggregated in the voids existing between the ionic parts which are not disrupted and keep their very short-range local order and in that sense exhibits a microphase-like separation.

Then, we have studied the spectra of carbon dioxide in the solution to obtain further clues about the interaction between the IL and its guest CO_2 molecules. A simple quantitative examination of the spectra of CO_2 in the region of its Fermi dyad (upper part of Figure 8) reveals the following trends. The doublet centered at 1277 and 1382 cm^{-1} at a CO_2 pressure of 0.11 MPa (molar fraction in the solution being approximately 0.16) is slightly blue-shifted, by about 1 cm^{-1} at the highest pressure investigated. The width (fwhh) of the upper component of the dyad is significantly greater than the experimental resolution (about 2.5 times) with a value about 4.3 cm^{-1} which is rather independent of the pressure. Finally, the ratio R of the intensity of the upper versus the lower component of the Fermi dyad is found to decrease slightly with the pressure from 4 to 2.4. These trends and the overall values of the observables are consistent with those that we have reported for the Fermi doublet of carbon dioxide diluted in organic solvents (e.g., benzene) in which this molecule interacts with the solvent to form heterodimers.[13−15] However, the band shape analysis performed in our earlier investigations, allowed us to show that the above treatment could be refined as each line of the dyad results from a weighted sum of two profiles. In this study, we indeed observe (Figure 8) that the lower component of the dyad is dissymmetric and presents a well-defined shoulder at lower frequency indicating that the band-shape is composite. Therefore, we have undertaken the same quantitative treatment of the dyad band-shape. We found that the best fitting procedure was obtained using two Lorentzian profiles to treat each line of the doublet (lower part of Figure 8). Using our earlier convention, we will denote the two fitted Lorentzian in the high frequency component of the Fermi doublet as U_1 and U_2 (U standing for upper). The label 1 (respectively 2) characterizes the fitted profile centered at the lowest frequency (respectively higher). This convention will be also applied to the lowest component of the Fermi dyad denoted L_1 and L_2 (L for lower).

The evolution with the CO_2 concentration of the band center positions of the peaks L_1 and L_2 and U_1 and U_2, their fwhh and the ratios $R = (I_{U_1} + I_{U_2})/(I_{L_1} + I_{L_2})$ and $R_2 = I_{U_2}/I_{L_2}$ where I denotes the integrated intensity of the Lorentzian lines, are

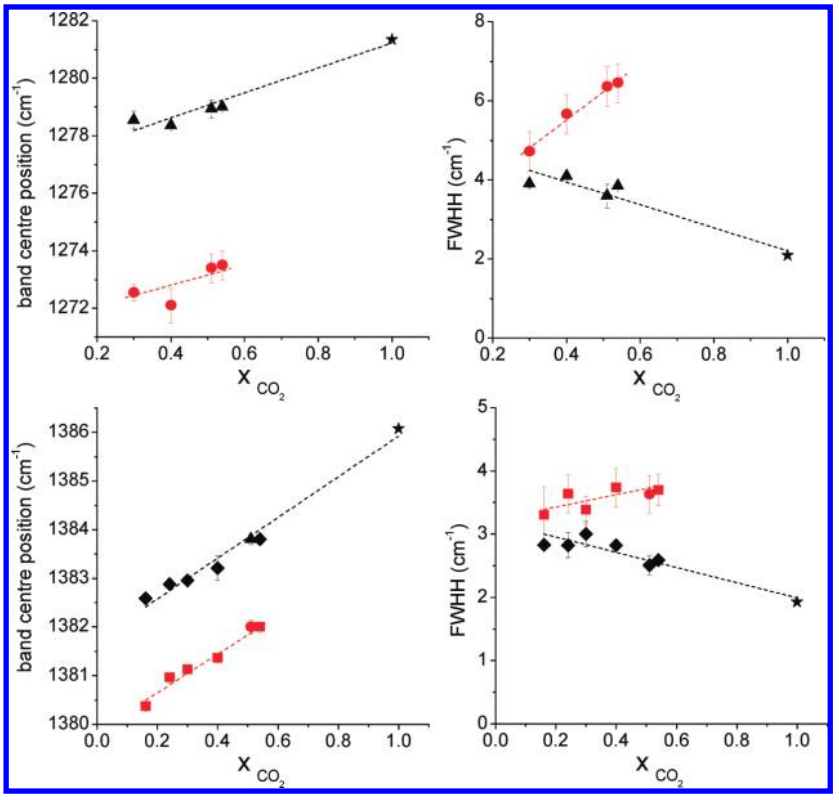

Figure 9. Evolution with the CO_2 concentration of the band center position (on the left) and of the fwhh (on the right) of the Lorentzian profiles (L_1 and L_2 lower and U_1 and U_2 upper components) fitted to the polarized Raman spectra in the CO_2 Fermi dyad domain of the mixtures at 313K (from $x_{CO_2} = 0.16$ up to 0.54, except for the L_1 and L_2 profiles of the lower component): (●) L_1, (▲) L_2, (■) U_1, and (♦) U_2. The value for pure CO_2 (22 MPa, ρ = 857.2 kg m^{-3}) is displayed for comparison (★).

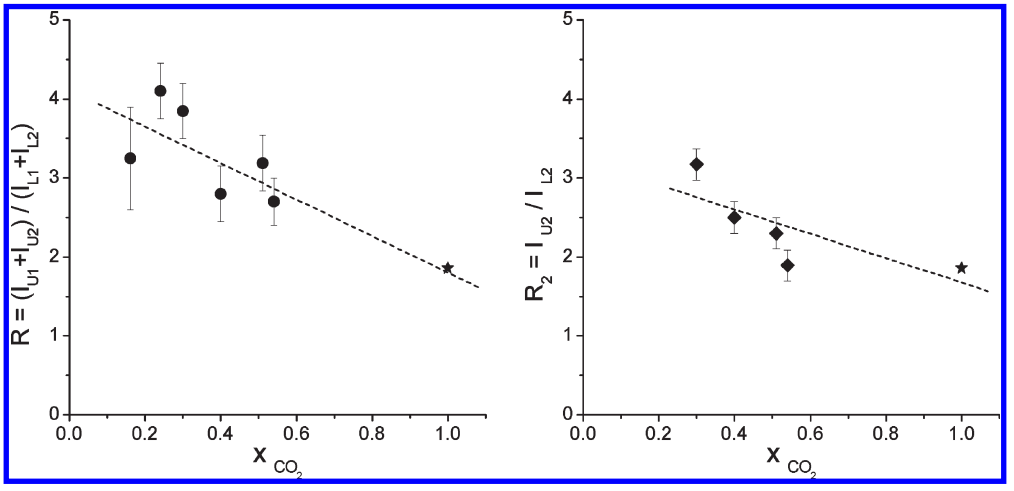

Figure 10. Evolution with the CO_2 concentration of the ratio of the integrated intensities I of the polarized Raman spectra in the CO_2 Fermi dyad domain of the mixtures at 313 K: on the left, $R = (I_{U_1} + I_{U_2})/(I_{L_1} + I_{L_2})$, on the right, $R = I_{U_2}/I_{L_2}$. The value for pure CO_2 (22 MPa, ρ = 857.2 kg m^{-3}) is displayed for comparison (★).

displayed in Figures 9 and 10, respectively. We found that the band center frequency values of the four fitted Lorentzian increase almost linearly with x_{CO_2} (Figure 9). We note that the difference between the values of the band centers of either the U_1 and U_2 profiles or the L_1 and L_2 profiles are almost constant but for the latter this difference is greater than for the former ones.

The values of the widths of the L_2 and U_2 profiles decrease with the CO_2 concentration in contrast to the trend observed on the L_1 and U_1 profiles. We also note that the widths of the upper components are smaller than those of the upper ones. Finally, we found that both ratios R and R_2 decrease continuously with increasing molar fraction of CO_2 (Figure 10).

The interpretation of the previous experimental data can be performed along the same line of reasoning that we have used in our precedent studies of the CO_2 solvent mixtures by taking into account the existence of transient complexes. In this

dx.doi.org/10.1021/jp111453a |J. Phys. Chem. B 2011, 115, 3538–3550

framework, the CO_2 molecules exist within two types of environments. In the first one (the so-called "free" environment) carbon dioxide molecules interact either with themselves or, in a "nonspecific" manner, with IL ions. In the second one (the so-called "bound" environment) CO_2 molecules interact "specifically" with the ions to form a transient heterodimer. On this ground, we have assigned the lower and upper Fermi components to carbon dioxide in the "free" environment as we did in earlier study using the fact that the values of the band center position associated with molecules in this site should reach in the limit of CO_2 molar fraction close to unity, those measured in pure CO_2 at a density close to that of the more concentrated mixture investigated ($x_{CO_2} = 0.54$). As seen in Figure 9 the evolutions of the band center values and of the fwhh of the L_2 and U_2 components with the CO_2 concentration in the mixture lead to extrapolated values in good agreement with those measured for pure CO_2 indicating that the L_2 and U_2 profiles should correspond to carbon dioxide in the "free" environment. Therefore, we are led to assign the L_1 and U_1 components to that of CO_2 "specifically" interacting with IL ions. We also note that the ratios of the integrated intensity R and $R_2 = I_{U_2}/I_{L_2}$ (Figure 9) extrapolated at $x_{CO_2} = 1$ lead to values which are close to that measured for pure CO_2. These observations are in agreement with those reported in our earlier studies.[13−15] We note that it is for the L_1 and U_1 profiles that the larger broadening is observed. This excess broadening compare to that of the L_2 and U_2 profiles may be certainly connected to the static and dynamic aspects involved in the chemical equilibria associated with the reaction leading to the formation of the complex. We raised also this issue in our earlier studies.[13] However, the lack of proper theory treating chemical exchange as seen from Raman profiles affected by a Fermi resonance and the technical difficulties associated in band-shape fitting using a large number of parameters which are rather difficult to assess a priori hamper us to proceed in a deeper analysis.

Nevertheless, it clearly comes out from the previous discussion that the trends and values of the features reveal that the behavior of carbon dioxide diluted in IL is similar to that observed for the solutions of this molecule in organic solvents.[13−15] As in former studies, we may infer that carbon dioxide molecules exist in two different environments (sites).

However, the opened question is now, with which species, namely the anion or the cation, the interaction takes place? Although there are no sizable signatures on the spectra of the IL, we indeed found a weak perturbation of the COO group of the anion. This observation would suggest that the main perturbation occurs on this moiety of the IL. The strength of the perturbations of the spectrum of carbon dioxide itself is revealed by the order of magnitude of the values of the shift and of the intensity ratio. These values are typical of a situation previously encountered for CO_2 interacting with an organic solvents in which a partial charge has been transferred from the electron donor center of the solvent molecule toward the carbon atom of CO_2 acting as an acceptor center.[13−15] We are finally led to conjecture at this level of the paper that such an interaction takes place between the COO group of Bmim TFA which are negatively charged and the positively charged carbon atom of CO_2. Considering the other site, we are thus led to the point of view that the IL offers sufficient free volume in the voids of the local structure existing among the different ion pairs to host carbon dioxide. In these sites, the CO_2 molecules interact among themselves without being too much disturbed.

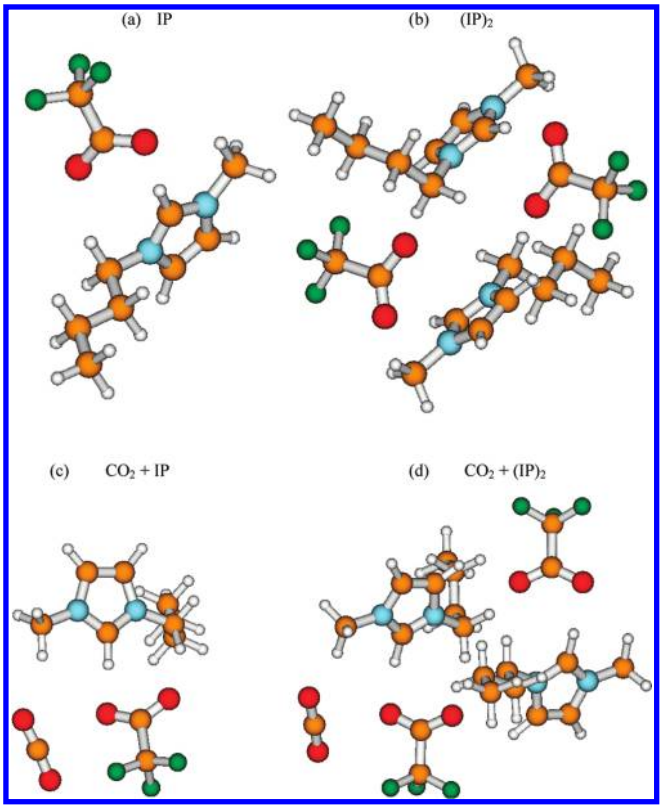

Figure 11. Structures of the IP and $(IP)_2$ without and with a molecule of CO_2 calculated at the B3LYP/6-31+G** level.

III. VIBRATIONAL MODELING USING DFT CALCULATIONS

Details of the Calculation. The quantum chemistry calculations have been carried out using the Gaussian 03 suite.[51] The optimized structures of the ion pair (IP) and a ion pair dimer $(IP)_2$ (with and without CO_2) have been achieved from the DFT procedure using the B3LYP functional using the 6-31+G(d,p) basis set. The optimized geometries have been obtained using a very tight criterion of convergence. The interaction energy values (ΔE_{int}) has been evaluated and corrected from the basis set superposition error (BSSE) according to the site−site function (SSFC) scheme.[52−56] Then, the vibrational analysis has been carried out from the calculated structures using the standard Wilson FG matrix formalism based on the harmonic force field approximation.[57]

Structures and Interaction Energy. In a first step, we have determined possible structures of the Bmim-TFA ion pair (IP) and ion pair dimer $(IP)_2$. Two calculated structures are displayed in Figure 11a,b. For a single IP the potential energy surface is extremely complicated and involves many local energy minimum structures. Among these latter, the global energy minimum structure has been retained for simplicity by neglecting the other secondary structures which could have comparable interaction energy values. However, the appearance of cooperative effects between ions leads us to consider that the ion pair dimer is certainly more realistic than the single pair as shown in our previous studies.[43,44] Even if the ion pair dimer remains undoubtedly an oversimplified picture of the structural organization in ILs, we could unambiguously determine an unique minimum energy structure. Other possible secondary structures, involving

Table 3. BSSE-Corrected Values of the Interaction Energy for the Calculated Structures of Ion Pair and Ion Pair Dimer Involving [CF_3COO^-] Anions with Bmim Cations with and without CO_2 [at the B3LYP/6-31+G(p,d) Level][a]

	ion pair (IP)			ion pair dimers $(IP)_2$	
		+CO_2			+CO_2
		Ionic Interactions			
ΔE_{int}(ions)	−88.2	−87.5	ΔE_{int}(ions)	−193.2	−192.9
			$\Delta E_{int}^{(2)}$	−217.7	−217.0
			$\Delta E_{int}^{(2)}$(Ca-An)	−313.4	−312.3
			$\Delta E_{int}^{(3)}$	+24.5	+24.1
		CO_2-Ion Interactions			
ΔE_{int}(CO_2-ions)		−3.9	ΔE_{int}(CO_2-ions)		−3.6
$\Delta E_{int}^{(2)}$		−5.7	$\Delta E_{int}^{(2)}$		−5.6
$\Delta E_{int}^{(2)}$(CO_2-TfA)		−5.1	$\Delta E_{int}^{(2)}$(CO_2-TfA)		−4.9
$\Delta E_{int}^{(3)}$		+1.8	$\Delta E_{int}^{(3)}$		+2.0
		Total Interaction Energy			
$\Delta E^{(cor)}_{int}$(TOT)	−88.2	−91.4		−193.2	−196.5
$\Delta E_{int}^{(cor+ZPE)}$(TOT)	n.c.	−90.8		n.c.	−196.0
ΔE_f(CO_2)		−3.2			−3.3
$\Delta H_f(T_{298K})$		−1.9			−2.6
$\Delta G_f(T_{298K})$		+5.6			+5.3

[a] Many-bodies interactions have been evaluated according to the SSFC scheme,[53,55] ΔE_{int} (ZPE) is the ZPE energy correction to the total interaction energy. $\Delta E_f(CO_2)$ is the association energy of CO_2. $\Delta H_f(T_{298K})$ and $\Delta G_f(T_{298K})$ are the corresponding enthalpy and Gibbs free energy (including thermal energy) calculated at T = 298 K and 0.1 MPa.

very different values of the interaction energy between ions, but which are less stable, are not presented here.

The BSSE-corrected values of the interaction energy for both IP and $(IP)_2$ structures have been reported in Table 3. For $(IP)_2$, the total interaction energy ΔE_{int}(TOT) is evaluated at −193.2 kcal/mol and mainly results from the pair interaction energy terms (∼−217.7 kcal/mol) between ions. The main stabilizing contribution due to the cation−anion pair interaction is evaluated at an average value about −78.4 kcal/mol for each of the cation−anion pairs. This value should be compared with −88.2 kcal/mol estimated for the single IP structure. The difference between these two values results from the electrostatic screening effect within the $(IP)_2$ structure due to the presence of surrounding ions (represented here by another coexisting cation−anion pair).

The calculated structures of CO_2 interacting with IP and with $(IP)_2$ are displayed in Figure 11c,d. In both structures, the C atom of CO_2 (Lewis acid center) interacts with one of the two O atoms of the TFA anion (Lewis base) with a separation distance $R_{C\cdots O}$ evaluated at about 2.78 and 2.80 Å, respectively. It is noteworthy that interacting with the TFA anion, CO_2 is found slightly deformed and bent, comparatively with the isolated linear structure, by an angle $\delta\alpha_{OCO}$ of about 4°. The average symmetry axis of the CO_2 molecule is tilted by an angle of about 38°−40° with respect to the anion plane (supposed here of C_{2v} symmetry by neglecting the CF_3 group). A brief survey of the calculated interaction energy values reported in Table 3 shows that the interaction energy between CO_2 and TFA is −5.0 kcal/mol. However, the presence of CO_2 has a minor influence on the stability between ions in the IP and the $(IP)_2$ structures (<1 kcal/mol). Therefore, the energy variation under the complex formation of CO_2 with either IP or $(IP)_2$ mostly results from the interaction of CO_2 with the ions. Nevertheless, non additive interactions represented by the 3-body terms ($\Delta E_{int}^{(3)}$) contribute to the repulsive terms in the interaction energy ΔE_{int}(CO_2-ions) and are evaluated at about 1.8−2.0 kcal/mol. Therefore, the association energy of CO_2 with the ion pairs ΔE_f(CO_2) is evaluated at about −3.3 kcal/mol from such a "gas phase model". In this framework, we have also reported in Table 3 the estimates of the enthalpy and free energy variations (calculated at 298 K and 1 atm.) for the complex formation with CO_2. Finally, the IP2 calculated structures (with and without CO_2) allow assessing the short-range organization within the polar network formed by ion species in Bmim TFA. In these structures, the pair of imidazolium cations forms a ring to ring stacking configuration slightly shifted to favor the insert of the TFA anions pair as well as to optimize the interaction energy between the different species. The symmetry axes (C_{2v} symmetry neglecting the CF_3 groups) of the anion pair are found with an antiparallel relative orientation. The axes lying along the CH bond of the imidazolium NC(H)N groups are also found in an antiparallel relative orientation. Such a short-ranged structure within the IP2 agrees with the conclusion obtained from the structural analysis of the simulated Bmim TFA.[58] In contrast, in our predicted IP2 structures, the butyl-chains of the two imidazolium rings are found situated at opposite extremities. In this arrangement, the cation dipole moments are found close to antiparallel configurations.

Vibrational Analysis. We have carried out the vibrational analysis of the predicted $(IP)_2$ structures (with and without CO_2) previously discussed. The main calculated (harmonic) fundamental transitions, IR and Raman Intensities (as well as the depolarization ratios) have been reported in Table 4. Clearly, the calculated IR and Raman lines associated with the main vibrational modes of both anions and cations of the $(IP)_2$ structures appear slightly perturbed by the presence of CO_2 interacting with one of the two TFA anions. However, we notice that the

Table 4. Vibrational Transitions, IR and Raman Intensities Associated with the Main Modes of the Bmim+ and CF_3COO^- Ions in the $(IP)_2$ and $CO_2 + (IP)_2$ Structures Calculated at the B3LYP/6-31+G Level**

	$(IP)_2$				$CO_2 + (IP)_2$			
assignment	ν_{calc} (cm^{-1})	I_{IR} (Km/mol)	I_{Ram} (Å^4/amu)	$\rho_{dep.}$	ν_{calc} (cm^{-1})	I_{IR} (Km/mol)	I_{Ram} (Å^4/amu)	$\rho_{dep.}$
b OCO (CO_2)					630.0	66.6	5.5	0.535
					656.5	21.1	inactive	0.491
b OCO	707.6	41.9	2.1	0.375	708.7	53.2	1.1	0.725
	708.3	46.1	3.4	0.036				
	708.9	1.9	4.3	0.145	709.8	16.2	3.7	0.061
ν_{CC}	819.6	75.7	5.2	0.069	821.0	66.9	3.5	0.101
	820.9	104.3	1.5	0.125	823.0	107.2	3.2	0.063
ν asym. op. CF (CF_3)	unresolved				unresolved			
					1156.3	134.9	0.9	0.507
ν asym.ip CF (CF_3)	1166.3	182.6	2.4	0.575	1156.7	107.3	1.5	0.737
	1169.8	283.0	2.2	0.483	1169.1	241.9	2.7	0.508
ν sym. CF (CF_3)	1203.8	632.4	1.0	0.132	1199.6	377.6	3.5	0.213
	1206.5	116.7	2.4	0.310	1205.6	296.8	1.8	0.369
ν sym CO (CO_2)					1363.3	2.4	25.3	0.086
ν sym COO	1430.8	96.9	14.7	0.481	1432.4	65.0	15.8	0.531
	1431.9	48.6	22.2	0.478	1434.0	62.0	33.5	0.424
ν asym C(CN) ring (R_2)	1606.4	66.6	0.6	0.128	1607.1	43.2	4.8	0.148
	1606.8	6.6	9.9	0.146	1608.8	13.1	6.8	0.124
ν sym C(CN) ring (R_1)	1612.8	58.2	0.7	0.236	1611.0	52.4	0.6	0.665
	1613.9	25.6	2.2	0.433	1614.3	32.1	1.9	0.463
ν asym COO	1716.0	0.9	7.7	0.731	1716.2	29.0	7.0	0.693
	1718.4	1313.5	inactive	0.739	1718.6	1385.4	0.2	0.387
ν asym CO (CO_2)					2409.7	628.6	0.3	0.738
ν asym C_2H (NC_2H)	3003.0	391.3	157.2	0.400	2991.2	560.4	133.9	0.397
	3013.3	770.2	70.8	0.384	3021.9	559.1	138.4	0.250
ν asym op $C_{(4,5)}H$ (HCCH)	3264.4	79.7	92.9	0.359	3262.2	100.3	89.8	0.354
	3267.0	106.7	64.2	0.375	3272.7	83.5	72.4	0.403
ν sym ip $C_{(4,5)}H$ (HCCH)	3303.1	3.8	118.5	0.177	3302.6	4.5	105.2	0.179
	3303.2	5.7	91.3	0.176	3303.6	6.1	108.1	0.162

calculated intensity of the IR line associated with the antisymmetric $\nu^{(as)}_{COO}$ stretching mode of TFA (ν_{calc} ~1716 and 1719 cm^{-1}), is slightly enhanced by about 8% under the influence of its interaction with CO_2. The Raman activity of the symmetric $\nu^{(s)}_{COO}$ mode of TFA (ν_{calc} ~ 1432 and 1434 cm^{-1}) is quite enhanced, by about 30%. This result agrees with the observed Raman features (see section II.2.2). It is noteworthy that the variation of the separation $\Delta\nu_{COO}=|\nu^{(as)}_{COO}-\nu^{(s)}_{COO}|$ between the $\nu^{(as)}_{COO}$ and the $\nu^{(s)}_{COO}$ stretching modes of TFA only decrease by less than 2 cm^{-1} under the complex formation of CO_2 with TFA. It is known that the value of $\Delta\nu_{COO}$ serves as a criterion to discuss the nature and strength of the interaction between the carboxylate group of the acetate anion with metals cations in aqueous solutions of salts.[37,59] The frequency separation is related to change in the CO bond lengths and to OCO angle of the carboxylate group and is strongly correlated with the interaction energy of the anion with the cations in different types of coordination. Thus, the variation of $\Delta\nu_{COO}$ of TFA can be considered as a spectral signature of the interaction of the anion TFA with its environment. The weak calculated value for $\Delta\nu_{COO}$ leads us to conclude that the polar network is weakly destabilized by the CO_2-complex formation with TFA. Incidentally, we notice that the νcc mode of TFA in the IP2 structures is almost unaffected by the presence of CO_2. Because, this mode is particularly sensitive to the complex formation of the carboxylate, this result confirms that CT interactions between CO_2 and TFA do not lead to sizable Raman spectral features. This is consistent with the findings discussed in section II.3.

We found that the degeneracy of the bending mode of CO_2 interacting with TFA is raised and leads to a splitting into two components separated by about 26.5 cm^{-1}. In Raman, the activity of this mode is induced by the interaction of CO_2 with its environment and therefore the corresponding band is expected to have a very weak activity with a rather broad band-shape. Unfortunately, experimentally, in the spectral domain of interest, the existence of two-well-defined strong bands assigned to modes of ILs (Figure 5a) hampers the detection of a possible weak and broad Raman bands due to the ν_2 bending mode of CO_2. However, we emphasize that it exists an entangled relationship between the splitting of the ν_2 bending mode of CO_2 and the spectral features observed in region of the Fermi resonance ($2\nu_2 - \nu_1$). Indeed, from the band-shape analysis discussed in section II.3, it is shown that both profiles of the dyad can be decomposed in two two-well-defined (L_1 and L_2) and (U_1 and U_2) components. The findings discussed in section II.3, concerning in particular the broadening of the (L_1 and U_1) components suggest that they are indeed related

dx.doi.org/10.1021/jp111453a |J. Phys. Chem. B 2011, 115, 3538–3550

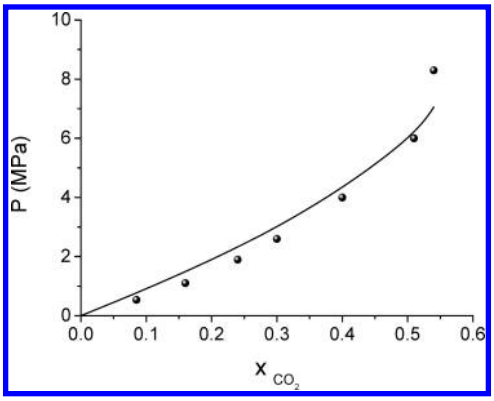

Figure 12. Carbon dioxide solubility in Bmim TFA. Solid line calculated assuming ideal liquid mixture.

with spectral features of CO_2 interacting quite specifically with TFA anions.

V. DISCUSSION AND CONCLUSION

The previous results have shown that the Bmim TFA IL is able to host a large amount of carbon dioxide without significant perturbation of its short-range local structure. This result presents some analogy with the segregation phenomenon reported in studies of IL.[60−62] It was shown that upon increasing the length of the alkyl chain, non polar domain become larger and more connected causing swelling of the ionic network.[50] Here, the role of the increasing alkyl chain is played by the increasing concentration of carbon dioxide. The system exhibits microphase-like separation in which the CO_2 molecules are mostly encountered aggregated in the voids existing between the ionic parts which are not disrupted and keep their very short-range local order. This result confirms how important the subdivision of short and long-range structure in IL is as reported by Schröder et al.[58]

We have provided evidence that the CO_2 guest molecules are perturbed as indicated by spectral signatures on its Fermi dyad. These perturbations are similar to that encountered for this molecule interacting through a charge transfer interaction mechanism with organic solvents. It is concluded from these findings that part of the CO_2 molecules resides in the void existing among the different ions pairs. In this "site", CO_2 molecules mostly interact among themselves. In the second "site", the carbon dioxide molecules (dynamically) coexist with the CO_2 molecule of the first site and interact more "specifically" via a CT interaction of the carbon atom of carbon dioxide with the negatively charged COO group of the TFA anion. The results presented here show this specific interaction to be weak and to engage only a small fraction of CO_2 molecules.

Finally, the picture at the molecular level of the CO_2 solvation in Bmim TFA can be discussed on thermodynamic grounds. Assuming as a working hypothesis that the mixture behaves as an ideal solution, we have calculated the solubility of CO_2 in the IL at 313 K using the Peng−Robinson equation of state to estimate the fugacity of the CO_2 in the gas phase. The calculated evolution of the pressure of CO_2 with its molar fraction in solution has been displayed in Figure 12 and compared with the experimental data taken from Table 1. In this figure it can be observed that up to a CO_2 concentration of 0.5 and a pressure of 6 MPa the solubility closely follows the ideal solution behavior described by the solid line. It is only at higher pressure that this analysis no longer holds as the gas−liquid equilibrium moves toward something akin to a liquid−liquid type of behavior.[20,63,64] The almost ideal behavior of the solubility can be physically understood by reminding that the CO_2−CO_2 interactions of molecules in the site 2 of the mixture are quite similar to those existing in pure CO_2 under the same thermodynamical conditions and that CO_2 interactions with the IL (belonging to site 1) are favorable and weak (Table 3 and reference). Moreover, it was found that the IL−IL interactions are essentially not perturbed by the presence of CO_2 (Table 3). All of these facts suggest that we are in the presence of a near athermal mixture where the excess enthalpies are very small. The solubility process could be dominated by entropic effects. However these are relevant only when the two compounds have significant differences in molar volumes. At 313 K, the CO_2 is very close to its critical point and its molar volume is half of the ionic liquid making the excess entropy of the system also small and conferring to the system a near ideal behavior.

AUTHOR INFORMATION

Corresponding Author

*Tel: +33 5 40006357. Fax: +33 5 4000 8402. E-mail: m.besnard@ism.u-bordeaux1.fr.

ACKNOWLEDGMENT

The authors are pleased to thank Drs. Jean Luc Bruneel and David Talaga for their help with the Raman experiments. We gratefully acknowledge the support provided by the M3PEC computer centre of the DRIMM (Direction des resources Informatiques et Multimédia Mutualisée, Talence, France) of the University of Bordeaux I and the IDRIS computer centre of the CNRS (Institut du Développement et des resources en Informatique Scientifique, Orsay, France) for allocating computing time and providing facilities. This work was partly funded by FCT under Project PTDC/EQU/FTT-102166/2008.

REFERENCES

(1) McHugh, M. A.; Krukonis, V. J. *Supercritical Fluid Extraction: Principles and Practice*; Butterworth-Heinemann: London, 1994.

(2) *Supercritical Fluids: Fundamentals and Application*; Kiran, E., Levelt-Sengers, J. M. H., Eds.; Kluwer Academic Publishers: Dordrecht, The Netherlands, 1994; Vol. 273.

(3) *Supercritical Fluids: Fundamentals and Application*; Kiran, E., Debenedetti, P. G., Peters, C. J., Eds.; Kluwer Academic Publishers: Dordrecht, The Netherlands, 2000; Vol. 366.

(4) Kajimoto, O. *Chem. Rev.* **1999**, *99*, 355.

(5) Tucker, S. C. *Chem. Rev.* **1999**, *99*, 391.

(6) Besnard, M.; Tassaing, T.; Danten, Y.; Andanson, J. M.; Soetens, J. C.; Cansell, F.; Loppinet-Serani, A.; Reveron, H.; Aymonier, C. *J. Mol. Liq.* **2006**, *125*, 88.

(7) Weingärtner, H. *Angew. Chem. Int. Ed.* **2008**, *47*, 654.

(8) Castner, E. W.; Wishart, J. F.; Shirota, H. *Acc. Chem. Res.* **2007**, *40*, 1217.

(9) Wasserscheid, P.; Welton, T. *Ionic Liquids in synthesis*, 2nd ed.; Wiley-VCH: Weinheim, Germany, 2004.

(10) Muldoon, M. M.; Aki, S. n. V. K.; Anderson, J. L.; Dixon, J. K.; Brennecke, J. F. *J. Phys. Chem. B* **2007**, *111*, 9001.

(11) Blanchard, L. A.; Gu, Z.; Brennecke, J. F. *J. Phys. Chem. B* **2001**, *105*, 2437.

(12) Kazarian, S. G.; Gupta, R. B.; Clarke, M. J.; Johnston, K. P.; Poliakoff, M. *J. Am. Chem. Soc.* **1993**, *115*, 11099.

(13) Besnard, M.; Cabaço, M. I.; Longelin, S.; Tassaing, T.; Danten, Y. *J. Phys. Chem. A* **2007**, *111*, 13371.
(14) Besnard, M.; Cabaço, M. I.; Talaga, D.; Danten, Y. *J. Chem. Phys.* **2008**, *129*, 224511.
(15) Besnard, M.; Cabaço, M. I.; Danten, Y. *J. Phys. Chem. A* **2009**, *113*, 184.
(16) Johnston, K. P.; Harrison, K. L.; Clarke, M. J.; Howdle, S. M.; Heitz, M. P.; Bright, F. W.; Carlier, C.; Randolph, T. W. *Science* **1996**, *271*, 624.
(17) McHugh, M. *Thermodynamics 2007*; Rueil-Malmaison, France, 2007.
(18) Melo, M. J. P.; Dias, A. M. A.; Blesic, M.; Rebelo, L. P. N.; Vega, L. F.; Coutinho, J. A. P.; Marrucho, I. M. *Fluid Phase Equilib.* **2006**, *242*, 210–219.
(19) Carvalho, P. J.; Coutinho, J. A. P. *J. Phys. Chem. Lett.* **2010**, *1*, 774.
(20) Carvalho, P. J.; Alvarez, V. H.; Schröder, B.; Gil, A. M.; Marrucho, I. M.; Aznar, M.; Santos, L. M. N. B. F.; Coutinho, J. A. P. *J. Phys. Chem. B* **2009**, *113*, 6803.
(21) Shiflett, M. B.; Kasprzak, D. J.; Junk, C. P.; Yokozeki, A. *J. Chem. Thermodyn.* **2008**, *40*, 25.
(22) Lalanne, P.; Rey, S.; Cansell, F.; Tassaing, T.; Besnard, M. *J. Supercrit. Fluids* **2001**, *19*, 199.
(23) Talaty, R.; Raja, S.; Storhaug, V. J.; Dölle, A.; Carper, W. R. *J. Phys. Chem. B* **2004**, *108*, 13177.
(24) Berg, R. W.; Deetlefs, M.; Seddon, K. R.; Shim, I.; Thompson, J. M. *J. Phys. Chem. B* **2005**, *109*, 19018.
(25) Rivera-Rubero, S.; Baldelli, S. *J. Phys. Chem. B* **2006**, *110*, 4756.
(26) Heimer, N. E.; Sesto, R. E. D.; Meng, Z.; Wilkes, J. S.; Carper, W. R. *J. Mol. Liq.* **2006**, *124*, 84.
(27) Holomb, R.; Martinelli, A.; Albinsson, I.; Lassègues, J. C.; Johansson, P.; Jacobsson, P. *J. Raman Spectrosc.* **2008**, *39*, 793.
(28) Jeon, Y.; Sung, J.; Kim, D.; Seo, C.; Cheong, H.; Ouchi, Y.; Ozawa, R.; Hamaguchi, H.-o. *J. Phys. Chem. B* **2008**, *112*, 923.
(29) Jeon, Y.; Sung, J.; Seo, C.; Lim, H.; Cheong, H.; Kang, M.; Moon, B.; Ouchi, Y.; Kim, D. *J. Phys. Chem. B* **2008**, *112*, 4735.
(30) Lassègues, J.-C.; Grondin, J.; Cavagnat, D.; Johansson, P. *J. Phys. Chem. A* **2009**, *113*, 6419.
(31) Wulf, A.; Fumino, K.; Ludwig, R. *J. Phys. Chem. A* **2010**, *114*, 685.
(32) Lassègues, J. C.; Grondin, J.; Cavagnat, D.; Johansson, P. *J. Phys. Chem. A* **2010**, *114*, 687.
(33) Robinson, R. E.; Taylor, R. C. *Spectrochim. Acta* **1962**, *18*, 1093.
(34) Christe, K. O.; Naumann, D. *Spectrochim. Acta* **1973**, *29A*, 2017.
(35) Agambar, C. A.; Orrell, K. G. *J. Chem. Soc. A* **1969**, 897.
(36) Baillie, M. J.; Brown, D. H.; Moss, K. C.; Sharp, D. W. A. *J. Chem. Soc. A* **1968**, 3110.
(37) Spinner, E. *J. Chem. Soc.* **1964**, 4217.
(38) *NIST Thermophysical Properties of Fluids Database*; NIST Standard Refere Data Program, NIST: Gaithersburg, MD, 2008.
(39) Nickolov, Z.; Ivanov, I.; Georgiev, G.; Stoilova, D. *J. Mol. Struct.* **1996**, *377*, 13.
(40) Quilès, F.; Burneau, A. *Vib. Spectrosc.* **1998**, *16*, 105.
(41) Quilès, F.; Burneau, A. *Vib. Spectrosc.* **1998**, *18*, 61.
(42) Frost, R. L.; Kloprogge, J. T. *J. Mol. Struct.* **2000**, *526*, 131.
(43) Danten, Y.; Cabaço, M. I.; Besnard, M. *J. Phys. Chem. A* **2009**, *113*, 2873.
(44) Danten, Y.; Cabaço, M. I.; Besnard, M. *J. Mol. Liq.* **2010**, *153*, 57.
(45) Fumino, K.; Wulf, A.; Ludwig, R. *Angew. Chem.* **2008**, *47*, 3830.
(46) Wulf, A.; Fumino, K.; Ludwig, R. *ChemPhysChem* **2010**, *47*, 349.
(47) Rodriguez, V.; Grondin, J.; Adamietz, F.; Danten, Y. *J. Phys. Chem. B* **2010**, *114*, 15057.
(48) Buffeteau, T.; Grondin, J.; Danten, Y.; Lassegues, J. C. *J. Phys. Chem. B* **2010**, *114*, 7587.
(49) Angenendt, K.; Johansson, P. *J. Phys. Chem. C* **2010**in press.
(50) Lopes, J. N. A. C.; Padua, A. A. H. *J. Phys. Chem. B* **2006**, *110*, 3330.
(51) Frisch, M. J.; Trucks, G. W.; Schlegel, H. B.; Scuseria, G. E.; Robb, M. A.; Cheeseman, J. R.; Montgomery, J. A.; Jr., T. V.; Kudin, K. N.; Burant, J. C.; Millam, J. M.; Iyengar, S. S.; Tomasi, J.; Barone, V.; Mennucci, B.; Cossi, M.; Scalmani, G.; Rega, N.; Petersson, G. A.; Nakatsuji, H.; Hada, M.; Ehara, M.; Toyota, K.; Fukuda, R.; Hasegawa, J.; Ishida, M.; Nakajima, T.; Honda, Y.; Kitao, O.; Nakai, H.; Klene, M.; Li, X.; Knox, J. E.; Hratchian, H. P.; Cross, J. B.; Adamo, C.; Jaramillo, J.; Gomperts, R.; Stratmann, R. E.; Yazyev, O.; Austin, A. J.; Cammi, R.; Pomelli, C.; Ochterski, J. W.; Ayala, P. Y.; Morokuma, K.; Voth, G. A.; Salvador, P.; Dannenberg, J. J.; Zakrzewski, V. G.; Dapprich, S.; Daniels, A. D.; Strain, M. C.; Farkas, O.; Malick, D. K.; Rabuck, A. D.; Raghavachari, K.; Foresman, J. B.; Ortiz, J. V.; A., Q. C.; Baboul, G.; Clifford, S.; Cioslowski, J.; Stefanov, B. B.; Liu, G.; Liashenko, A.; Piskorz, P.; Komaromi, I.; Martin, R. L.; Fox, D. J.; Keith, T.; Al-Laham, M. A.; Peng, C. Y.; Nanayakkara, A.; Challacombe, M.; Gill, P. M. W.; Johnson, B.; Chen, W.; Wong, M. W.; Gonzalez, C.; Pople, J. A. Gaussian 03; Gaussian Inc.: Wallingford, CT, 2004.
(52) Boys, S. F.; Bernardi, F. *Mol. Phys.* **1970**, *19*, 553.
(53) Mierzwicki, K.; Latajka, Z. *Chem. Phys. Lett.* **2003**, *380*, 654.
(54) Tury, L.; Dannenberg, J. J. *J. Phys. Chem.* **1993**, *97*, 2488.
(55) Valiron, P.; Mayer, I. *Chem. Phys. Lett.* **1997**, *1997*, 46.
(56) White, J. C.; Davidson, E. R. *J. Chem. Phys.* **1990**, *93*, 8029.
(57) Wilson, E. B.; Decius, J. C.; Cross, P. C. *Molecular Vibrations*; McGraw-Hill, New York, 1955.
(58) Schröder, C.; Rudas, T.; Neumayr, G.; Gansterer, W.; Steinhauser, O. *J. Chem. Phys.* **2007**, *127*, 44505.
(59) Nara, M.; Torii, H.; Tasumi, M. *J. Phys. Chem.* **1996**, *100*, 19812.
(60) Shigeto, S.; Hamaguchi, H. *Chem. Phys. Lett.* **2006**, *427*, 329.
(61) Triolo, A.; Russina, A.; Bleif, H. J.; Cola, E. D. *J. Phys. Chem. B* **2007**, *111*, 4641.
(62) Russina, O.; Triolo, A.; Gontrani, L.; Caminiti, R.; Xiao, D.; L. G. H., Jr; Bartsch, R. A.; Quitevis, E. L.; Plechkova, N.; Seddon, K. R. *J. Phys.: Condens. Matter* **2009**, *21*, 414221.
(63) Carvalho, P. J.; Alvarez, V. H.; Machado, J. J. B.; Pauly, J.; Daridon, J.-L.; Marrucho, I. M.; Aznar, M.; Coutinho, J. A. P. *J. Supercrit. Fluids* **2009**, *48*, 99.
(64) Carvalho, P. J.; Alvarez, V. H.; Marrucho, I. M.; Aznar, M.; Coutinho, J. A. P. *J. Supercrit. Fluids* **2010**, *52*, 258.